SPE 29110

# Ninth SPE Comparative Solution Project: A Reexamination of Black-Oil Simulation

J.E. Killough, U. of Houston

SPE Member



This paper was prepared for presentation at the 13th SPE Symposium on Reservoir Simulation held in San Antonio, TX, U.S.A., 12-15 February 1995.



## Abstract

The Ninth SPE Comparative Solution Project presented in the following paper provides a reexamination of black-oil simulation based on a model of moderate size (9,000 cells) and with a high degree of heterogeneity provided by a geostatistically-based permeability field. Nine participants provided data for the comparison which is based on a dipping reservoir with twenty-five somewhat randomly placed producers and a single water injector.

Results showed that significant agreement could be achieved for this problem on the basis of total production rates, saturations, and reservoir pressures. On the other hand, rates for some individual wells did show variations of as much as 30% due to differing treatments of well flowing bottomhole pressures. All participants were able to simulate the study in fewer than sixty time-steps with an average of 4-5 Newton iterations per step. In addition, the results showed that this moderate-sized problem could be simulated in only a few minutes in a workstation environment for the two plus years of data.

## Introduction

The SPE Comparative Solution Projects[1-8] have to this date comprised studies over the past fifteen years which involved varying aspects of reservoir simulation. The first two comparative solution projects focused on black-oil simulation for Cartesian and radial grid geometries. More recent studies have been devoted to specialized simulations such as compositional, dual porosity, thermal, and miscible; or they have looked at treatment of horizontal wells and gridding.

The purpose of the current project is two-fold: to provide an update to previous black-oil based projects and to investigate the complications brought about by a the high degree of heterogeneity in a geostatistically-based permeability field.

## Description of the Reservoir Simulators

From the first comparative solution project to the present, the capabilities of black-oil reservoir simulators have increased tremendously. Currently, the linear equation solutions are generally performed by a preconditioned conjugate-gradient-like method such as incomplete LU factorization preconditioned ORTHOMIN. These solvers have predominantly replaced techniques such as SIP and LSOR for the more difficult non-symmetric cases resulting from highly-heterogeneous and fully-implicit solutions. Well treatments have become more sophisticated with almost all simulators providing some form of treatment of implicit bottomhole pressures for rate constrained wells. Finally, because of the sophistication of the linear solvers and the power of

References and illustrations at end of paper current workstations, the use of fully-implicit solutions for added stability has become more widespread for even large field-wide simulations.

The following paragraphs describe the reservoir simulators which were used in the project by the various participants.

**AEA Technology**

The TechSIM simulator of AEA technology was used for this work. This is an in-house simulator used for reservoir engineering consultancy in AEA Technology. It uses a generalized compositional model and includes options for black oil, miscible flood and equation of state compositional simulation. The run for this project used a fully implicit solution. The linear solver was Orthomin with a nested factorization pre-conditioner. Stone's model 2 was used for 3 phase relative permeabilities.

The simulator formulation is described in reference 9.

**ARCO**

ARCO's in-house, black-oil simulator employs IMPES and fully implicit techniques for time step discretizations. A selective implicit option is available when employing local grid refinement. Nonlinear equations are solved for implicit problems using Newton-Raphson combined with a line search technique. Linear equations are solved using various pre-conditioned conjugate gradient-like techniques.

The comparison problem was run using the fully implicit option. Time step targets of 200 psi and 5% were used for pressure and saturation changes, respectively. A five day time step was taken immediately following the rate changes at 300 and 360 days. The linear equations were solved using a constrained pressure residual technique combined with a nested factorization technique. The linear solver used for this problem was developed by John Wallis of Western Atlas Software[10].

**CMG**

CMG's black-oil model IMEX was used for the ninth SPE comparative problem. IMEX is an adaptive-implicit black-oil, field scale model with a pseudo-miscible/polymer option. The simulator has many features such as dual porosity/dual permeability, well management capabilities and several initialization options. The flow equations are solved using a sparse matrix solver which can be run in iterative or direct mode. The iterative technique used is the standard ILU with GMRES acceleration. All wells are fully coupled.

**INTERA Information Technologies**

ECLIPSE 100 is a flexible and widely used general purpose commercial black-oil simulator with gas condensate options. A range of modelling facilities make it applicable to most of the worlds petroleum reservoirs. The use of robust numerical techniques and fully implicit technology ensures that full field and well coning studies are solved accurately and efficiently with minimum residual and material balance errors, so that ECLIPSE is very suitable for modelling heterogeneous reservoirs exemplified by this comparison problem.

ECLIPSE 100 possesses a range of facilities for modelling of aquifers, fractured reservoirs, segregated flows and incorporates a generalised tracer tracking facility. A wide range of rock and relative permeability models including hysteretic and irreversible descriptions honour the physical characterisation of most reservoirs. ECLIPSE has a comprehensive set of options for controlling individual wells and group hierarchies to match various production and injection constraints and economic limits and to abet the history matching process.

**SENSOR**

Sensor is a three-dimensional, three-phase reservoir simulation model for black-oil and compositional applications[11]. Both IMPES and fully-implicit formulations are included. The model's use of a relaxed volume balance concept effectively conserves both mass and reduces Newton iterations. A new implicit well rate calculation method improves IMPES stability. It approximates wellbore crossflow effects with high efficiency and relative simplicity in both IMPES and fully-implicit simulations. Multiphase flow in tubing, gas lift, and near-well turbulent gas flow effects are treated implicitly.

Initial saturations are calculated as a function of water-oil and gas-oil capillary pressures which are optionally dependent upon the Leverett J-function. A normalization of the relative permeability and capillary pressure curves is used to calculate these terms as a function of rock type and grid block residual saturations.

## SSI

Scientific Software-Intercomp's SIMBEST II is a fully implicit simulator, which simulates conventional black oil reservoirs, dual porosity reservoirs and pseudo-compositional modeling of retrograde condensates, gas cycling and volatile oils, and miscible gas injection. It is designed to solve problems involving as many as three fluid phases and five components in dual and/or single porosity mode.

This problem was solved using the ESPIDO iterative linear solution package, with solution methods and preconditioners selected automatically by the ESPPSA package. The time stepping sequence and tolerances were determined automatically by SIMBEST.

Results reported by Fina in the latter part of this article also used the SIMBEST II simulator.

## TIGRESS

The TIGRESS simulator is based on a generalized compositional formulation which incorporates IMPES and fully-implicit solution techniques. Fluid properties can be calculated using either black-oil or equation-of-state compositional models. The non-linear equations are solved by Newton's method. Linear equations are solved either by Line Successive Over Relaxation or by ORTHOMIN with nested factorization preconditioner.

## WESTERN ATLAS SOFTWARE

DESKTOP-VIP is a full-featured reservoir simulation software system for Unix workstations, linking a graphical user interface with VIP-EXECUTIVE, a comprehensive suite of reservoir simulation software. VIP-EXECUTIVE is a multi-component, three dimensional, three phase reservoir simulator which contains a number of modules sharing a common compositional formulation. VIP-EXECUTIVE offers both fully implicit and IMPES model formulations of the differential equations governing conservation and flow in the reservoir. A variety of matrix solution methods are provided for use with both formulations, including both direct and iterative procedures. In general, the most efficient solution method is a proprietary solver, BLITZ, which uses residual constraints combined with preconditioned generalized minimum residual acceleration (GMRES) to substantially reduce both work and storage requirements.

# Problem Description

The reservoir description for the Ninth Comparative Solution Project was based on a 24x25x15 grid placed on a dipping reservoir. To ease the amount of data input required of the participants, a dataset from one of the participants (VIP) was supplied for the problem. The grid was in conventional rectangular coordinates without corner point geometry or local grid refinement. The dimensions of the grid blocks are 300 feet in both the X- and Y-directions. Cell (1,1,1) is at a depth of 9000 feet subsea at the center of the cell top. The remaining cells dip in the X-direction at an angle of 10 degrees. There is no dip in the Y-direction. The values of porosity and thickness for each layer in the model[2] are constant as shown in the following Table:

**Table 1**
**Layer Porosity and Thickness Values**

| Layer | Porosity | Thickness (feet) |
|---|---|---|
| 1 | 0.087 | 20 |
| 2 | 0.097 | 15 |
| 3 | 0.111 | 26 |
| 4 | 0.16 | 15 |
| 5 | 0.13 | 16 |
| 6 | 0.17 | 14 |
| 7 | 0.17 | 8 |
| 8 | 0.08 | 8 |
| 9 | 0.14 | 18 |
| 10 | 0.13 | 12 |
| 11 | 0.12 | 19 |
| 12 | 0.105 | 18 |
| 13 | 0.12 | 20 |
| 14 | 0.116 | 50 |
| 15 | 0.157 | 100 |

Values for PVT properties for the Oil and gas were also based on the Second Comparative Solution Project[2] and are give in Table 2:

**Table 2**
**PVT Properties for the Oil and Gas Phases**

| Psat | Rs | Bo | Zg | Gr | Vo | Vg |
|---|---|---|---|---|---|---|
| 4000 | 1500 | 1.1200 | .8300 | .92 | .94 | .0175 |
| 3600 | 1390 | 1.1100 | .8299 | .92 | .95 | .0170 |
| 3200 | 1270 | 1.0985 | .8398 | .92 | .98 | .0165 |
| 2800 | 1130 | 1.0870 | .8341 | .92 | 1.00 | .0160 |
| 2400 | 985 | 1.0750 | .8341 | .92 | 1.03 | .0155 |
| 2000 | 828 | 1.0630 | .8370 | .92 | 1.06 | .0150 |
| 1600 | 665 | 1.0510 | .8341 | .92 | 1.08 | .0145 |
| 1200 | 500 | 1.0380 | .8341 | .92 | 1.11 | .0140 |
| 800 | 335 | 1.0255 | .8370 | .92 | 1.14 | .0135 |
| 400 | 165 | 1.0120 | .8369 | .92 | 1.17 | .0130 |
| 14.7 | 0 | 1.0000 | .9999 | .92 | 1.20 | .0125 |

where,

| | |
|---|---|
| Psat | = saturation pressure (psia) |
| Rs | = solution gas/oil ratio(SCF/STB) |
| Bo | = formation volume factor (RB/STB) |
| Zg | = gas Z value |
| Gr | = gas gravity |
| Vo | = oil viscosity |
| Vg | = gas viscosity |

Relative permeabilities and capillary pressure functions are shown in Figures 1 and 2. The interesting feature in the water-oil capillary pressure curve is the discontinuity at about 35% water saturation. This data was taken from an actual production reservoir study being performed by an oil company. The discontinuity can lead to difficulties in Newton Raphson convergence for cases in which water saturations are changing significantly. The second feature of the capillary pressure curve is the tail which does not extend to a water saturation of 1.0. Although unusual, this feature does represent reality in certain reservoirs in which imbibition may have occurred due to techtonics prior to discovery.

Gas-oil saturation functions were given in the following table also from the Second Comparative Solution Project:

**Table 3**
**Saturation Functions for the Gas-Oil System**

| Sg | krg | krog | Pcgo |
|---|---|---|---|
| 0 | 0 | 1. | 0 |
| 0.04 | 0.0 | 0.6 | 0.2 |
| 0.1 | 0.022 | 0.33 | 0.5 |
| 0.2 | 0.1 | 0.1 | 1.0 |
| 0.3 | 0.24 | 0.02 | 1.5 |
| 0.4 | 0.34 | 0.0 | 2.0 |
| 0.5 | 0.42 | 0.0 | 2.5 |
| 0.6 | 0.5 | 0.0 | 3.0 |
| 0.7 | 0.8125 | 0.0 | 3.5 |
| 0.88491 | 1.0 | 0.0 | 3.9 |

The initial reservoir temperature is 100 degrees F with an initial oil phase pressure of 3600 psia at a depth of 9035 feet subsea. The saturation pressure of the oil is 3600 psia. For cells with oil pressures less than this value the saturation pressure is set equal to the oil phase pressure. At 1000 psi above the saturation pressure the Bo is 0.999 times that of the Bo at Psat. The oil viscosity does not increase with increasing pressure in undersaturated conditions. The density of the stock tank oil is 0.7206 gm/cc and the molecular weight of the residual oil is 175. The oil pressure gradient is approximately 0.3902 psi/ft at 3600 psia. The stock tank water density is 1.0095 gm/cc with a water formation volume factor (Bw) at 3600 psia of 1.0034 RB/STB yielding a water pressure gradient of approximately 0.436 psi/ft.

The oil-water contact is 9950 feet subsea. The water saturation distribution is calculated based on the oil-water capillary pressure curve. Because of the lack of data above Sw=0.88149 a small residual oil saturation exists throughout the modeled reservoir. There is no free gas initially in the reservoir.

With these data, initialization of the model produced a water saturation distribution as shown in Figure 3. The input data included in the distribution to the participants included a geostatistically generated permeability field on a cell by cell basis. The distribution of the data on the grid is shown in Figure 5. Figure 4 is a semi-variogram of the data showing the correlation length in the X-direction to be about 1800 feet or six grid blocks. There is no correlation of the data in either the Y- or Z-directions.

A total of twenty-five producers and 1 water injection well were included in the modeled reservoir. The maximum oil rate for all producers was set at 1500 STBO/D at time zero. At 300 days this rate was lowered to 100 STBO/D for all wells. Finally, at 360 days the rate was again raised to 1500 STBO/D for all producers until the end of the simulation at 900 days. The minimum flowing bottomhole pressure was set to 1000 psia for all producers with a reference depth of 9110 feet for this pressure in all wells. The water injector was set to a maximum rate of 5000 STBW/D with a maximum bottomhole pressure of 4000 psia at a reference depth of 9110 feet subsea. All producers were completed in layers 2,3, and 4 only and the water injector was completed in layers 11, 12,13,14, and 15. Well productivity/injectivity indices were calculated with a wellbore radius of 0.5 feet, a drainage radius of 60 feet (0.2*DX) and zero skin.

The producing well distribution is shown in Figure 6. The water injection well is located areally at grid block (24,25) in the corner of the grid.

Also shown in Figure 6 is the gas saturation distribution at the end of simulation (900 days). The unusual distribution of gas saturations is the result of the high degree of heterogeneity provided by the permeability distribution. The gas saturation began forming shortly after the beginning of the simulation (about 100 days) when the reservoir pressure is reduced significantly below the original saturation pressure and gas percolates to the top of the reservoir.

## Results

Before presenting the results of the participants, it is instructive to understand the performance of the model for various operating conditions. Table 4 lists the time step comparison for one of the models for a standard IMPES run with no implicit treatment of wells and for a fully-implicit simulation.

**Table 4**
**Comparison of IMPES and Fully-Implicit Simulations**

| Formulation | Time Steps | Newton Iterations |
|---|---|---|
| IMPES | 2180 | 2180 |
| Fully-Implicit | 27 | 109 |

Clearly, from these data it appears that due to the stability limitations caused by gas percolation, the IMPES time steps were severely limited. A comparison of the IMPES case with the fully-implicit case using 60 day (above) and 10 day maximum time step does indicate that there is some time truncation error associated with the simulation as shown in Figure 7 for the field GOR versus time. Total variation of GOR is almost 10% depending on the maximum time step in the simulation. For the majority of the cases, smaller time steps in the IMPES case lead to higher values of GOR. Because of these observed variations with the same simulator, it was likely that some variation was to be expected from the participants' results.

Participants were asked to report results for the simulation in several ways. The primary data which were collected were the field total producing rates for oil, gas, and water. Figure 8 shows a three-dimensional plot of the field oil rates for all participants. The variation of field oil rates is within 9% of the mean value for all participants. Figure 9 shows the field gas rate as a function of time for all participants. The variation is slightly larger than in the case of the oil rates with the maximum deviation being about 11% of the mean value. The water rate for all participants varied considerably as shown in Figure 10. Maximum deviation after about 100 days was on the order of 20%. The main reason for this probably lies in the treatment of relative permeabilities and capillary pressures. Use of Stone's Model I 3-phase relative permeabilities as opposed to the Stone II model used by most of the participants results in a higher water production rate. Similarly, initialization with 100% water saturation in the aquifer area, as used by some of the participants, also caused higher water production.

Due to the high compressibility of the model's secondary gas cap, reservoir pressures for all participants showed small deviations as shown in Figure 11. Maximum deviation was about 4%. Similarly, gas saturations in the secondary gas cap at location (1,13,1) in the center of the top of the model showed only a 5% variation as illustrated in Figure 12.

Water saturations near the bottom of the row of producers again showed some larger variations due to treatment of relative permeability and capillary pressures. As shown in Figure 13, near the end of the simulation the variation in water saturation is about 25% among the participants. Variations may also have been due to the amount of water injection allowed due to bottom hole pressure constraint. As shown in Figure 14, these injection rates varied considerably due to conditions in the aquifer (i.e., use of 100% water saturation).

Finally, Figure 15 plots the oil production rate for well 21 located in cells (8,20,2), (8,20,3), and (8,20,4). As shown in this figure the variation in oil rate is quite large for two of the participants. From the change in oil rate after the 360 day period, it appears that the treatment of well index (or productivity index) may be different for the simulations which show higher oil rates than the average. With the exception of these two results, the data for well 21 from the other participants agreed to within about 4% duplicating the results of the other data previously described.

Finally, the participants provided data concerning the number of time steps, non-linear iterations and CPU time associated with the model simulations. Table 5 summarizes these results. Since participants optimized simulations to differing degrees, the comparison of this data should only be taken as qualitative.

**Table 5**
**Comparison of Time Step Data**

| Participant | Time Steps | Outer It. | CPU(s) |
|---|---|---|---|
| AEA | 57 | 200 | 391[a] |
| | 57 | 200 | 3720[b] |
| ARCO | 31 | 98 | 181[c] |
| CMG | 48 | 256 | 1122[d] |
| ECLIPSE | 31 | 142 | 207[c] |
| | 31 | 142 | 535[d] |
| SENSOR | 33 | 55 | 102[c] |
| SSI | 34 | 95 | 427[e] |
| TIGRESS | 46 | 194 | 810[f] |
| VIP | 27 | 109 | 141[c] |

a = IBM R/S 6000/3AT
b = SUN Sparcstation 2
c = IBM R/S 6000/590 (xlf 3.1)
d = HP 735
e = IBM R/S 6000/370 (xlf 2.3)
f = IBM R/S 6000/365

Although it is difficult to draw conclusions from this data, there are two observations which can be made. First, the formulation in the SENSOR program does allow a significant reduction in the total number of Newton iterations required to solve the problem. Secondly, the CPU times for the workstations reported by the participants, and especially the IBM R/S 6000/590, indicate the simulation of this moderate-sized problem can be accomplished in only a few minutes of computing time.

## Conclusions

This article has presented the model and the results for the Ninth SPE Comparative Solution Project. The data used for the model attempted to bring into the comparative solution project a model of moderate size (9,000 finite difference cells) and with a high degree of heterogeneity provided by a geostatistically-based permeability field. Results provided by the participants showed a remarkable degree of agreement with maximum variations in field oil rates and gas saturations of less than ten percent. The major difference among the results was the oil production rate of well 21. This apparently was due to differing treatments of well indices among the participants.

It is hoped that this comparison will provide a more up-to-date basis for the validation of new models and formulations as they are developed in the future. A detailed version of the data presented here is available from the author (e-mail johnk@uh.edu).

## Acknowledgment

The author wishes to express his appreciation to the participants for providing the data and manpower for the results presented in this study.

## References

1. Odeh, A., "Comparison of Solutions to a Three-Dimensional Black-Oil Reservoir Simulation Problem", *JPT* , Vol. 33, January 1981, pp.13-25.

2. Weinstein, H.G., Chappelear, J.E., and Nolen, J. S., "Second Comparative Solution Project: A Three-Phase Coning Study," *JPT*, Vol. 38, March 1986, pp. 345-353.

3. Kenyon, D.E. and Behie, G. A., "Third SPE Comparative Solution Project: Gas Cycling of Retrograde Condensate Reservoirs," *JPT*, Vol. 39, August 1987, pp. 981-998.

4. Aziz, K. Ramesh, A.B., and Woo, P.T., "Fourth SPE Comparative Solution Project: A Comparison of Steam Injection Simulators," *JPT*, Vol. 39, December 1987, pp. 1576-1584.

5. Killough, J., and Kossack, C., "Fifth SPE Comparative Solution Project: Evaluation of Miscible Flood Simulators," SPE 16000 presented at the Ninth SPE Symposium on Reservoir Simulation, San Antonio, Texas, February 1-4, 1987.

6. Firoozabadi, A., and Thomas, L. K., "Sixth SPE Comparative Solution Project" Dual-Porosity Simulators," *JPT*, Vol. 42, June 1990, pp. 710-715 and 762-763.

7. Ngheim, L., Collins, D.A., and Sharma, R., "Seventh SPE Comparative Solution Project: Modeling of Horizontal Wells in Reservoir Simulation," SPE 21221 presented at the Eleventh SPE Symposium on Reservoir Simulation, Anaheim, California, February 17-20, 1991.

8. Quandalle, P., "Eighth SPE Comparative Solution Project: Gridding Techniques in Reservoir Simulation," SPE 25263 presented at the Twelfth SPE Symposium on Reservoir Simulation, New Orleans, February 28-March 3, 1993.

9. Mott, R.E. and Farmer, C.L., "A New Formulation for Generalized Compositional Simulation," Proceedings of the 2nd European Conference on the Mathematics of Oil Recovery, Arles, France, September 11-14 1990, pp339-342.

10. Wallis, J. R., Kendall, R.K., and Little, T., "Constrained Residual Acceleration of Conjugate Residual Methods," SPE 13536 presented at the Eighth SPE Symposium on Reservoir Simulation, Dallas, Texas, February 10-13, 1985.

11. Coats, K.H., Thomas, L. K., and Pierson, R. G., "Compositional and Black-Oil Reservoir Simulation," SPE 29111 presented at the Twelfth SPE Symposium on Reservoir Simulation, San Antonio, Texas, February 12-15, 1995.

**Figure 1: Water-Oil Capillary Pressures**

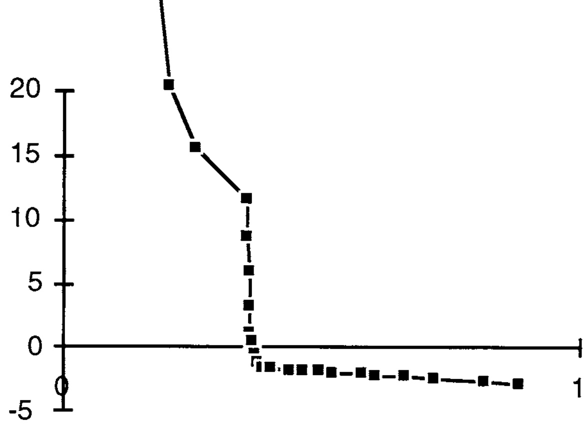


**Figure 2: Water and Oil Relative Permeabilities**

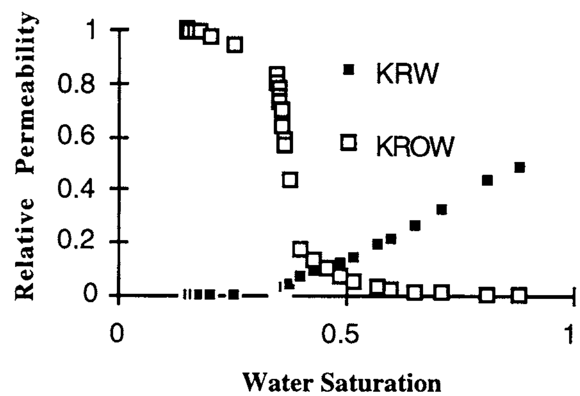


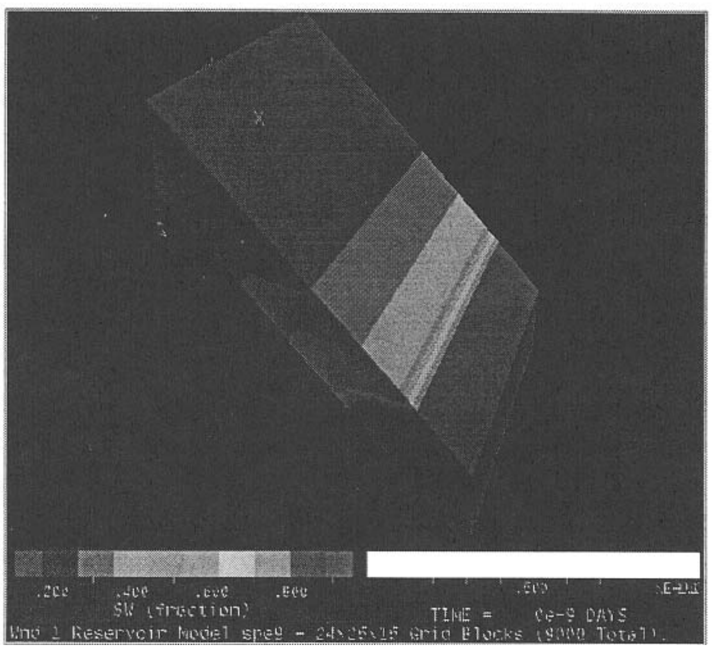


**Figure 3:**
**Initial Water Saturation**
**of Reservoir**

**Figure 4: Semi-Variogram of Permeability Distribution**

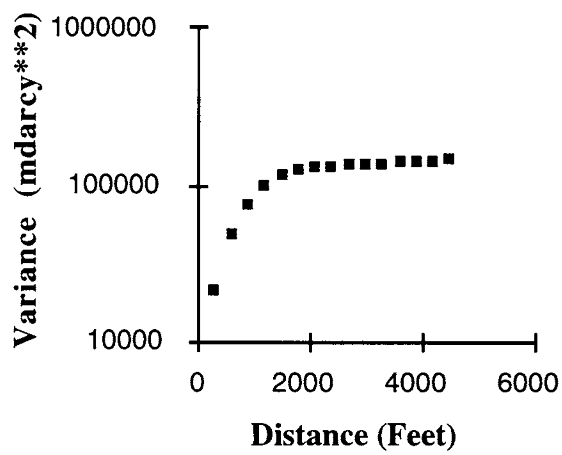

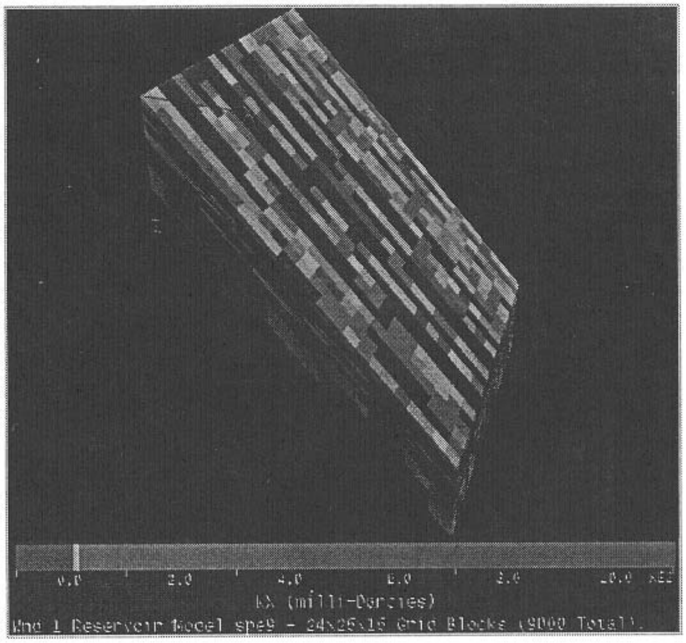


**Figure 5:**
**Permeability Distribution**
**for the Reservoir**

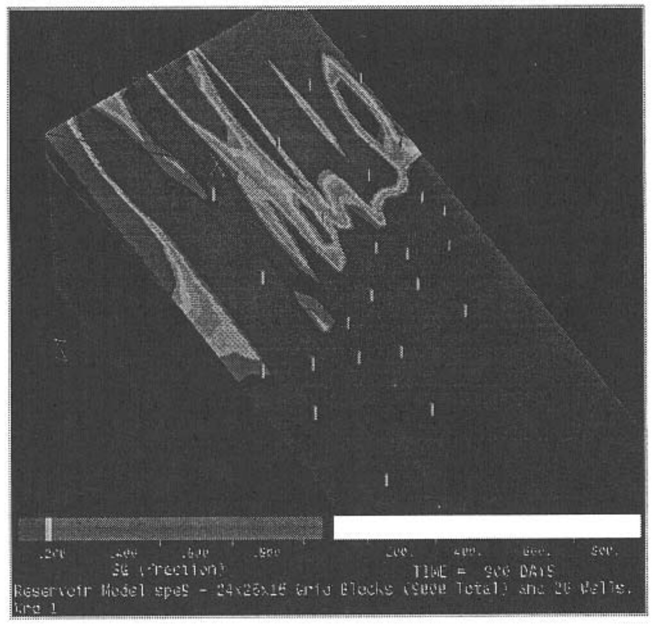


**Figure 6: Gas Saturations at 900 Days**

**Figure 7: Variation of GOR With Time Step**

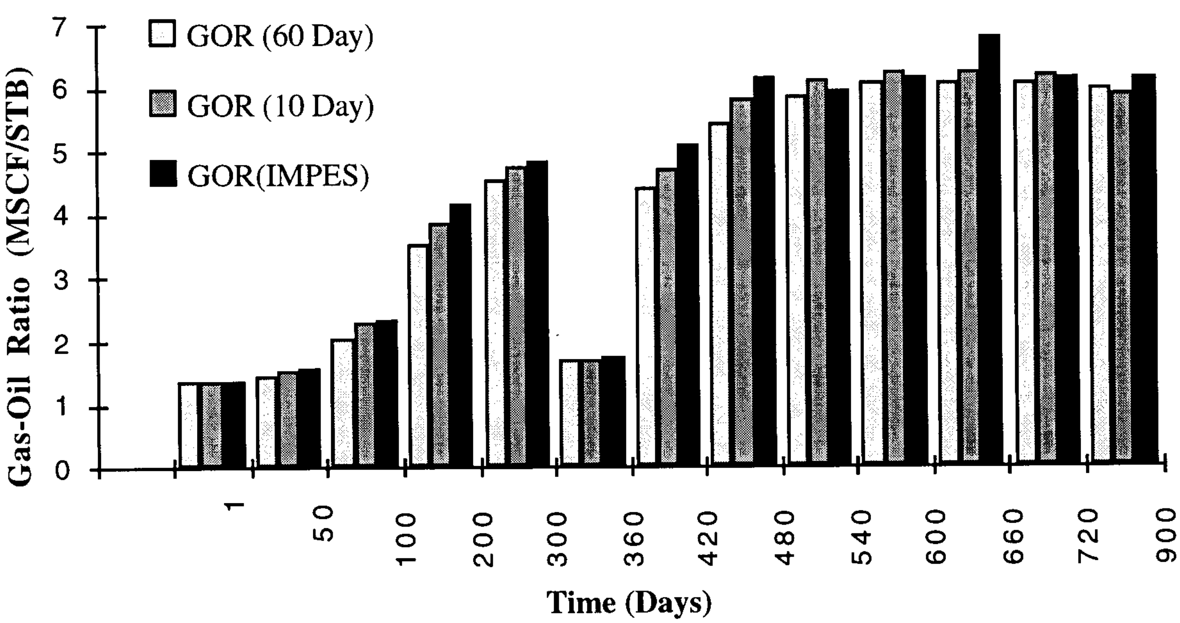

**FIGURE 8: COMPARISON OF FIELD OIL RATES**

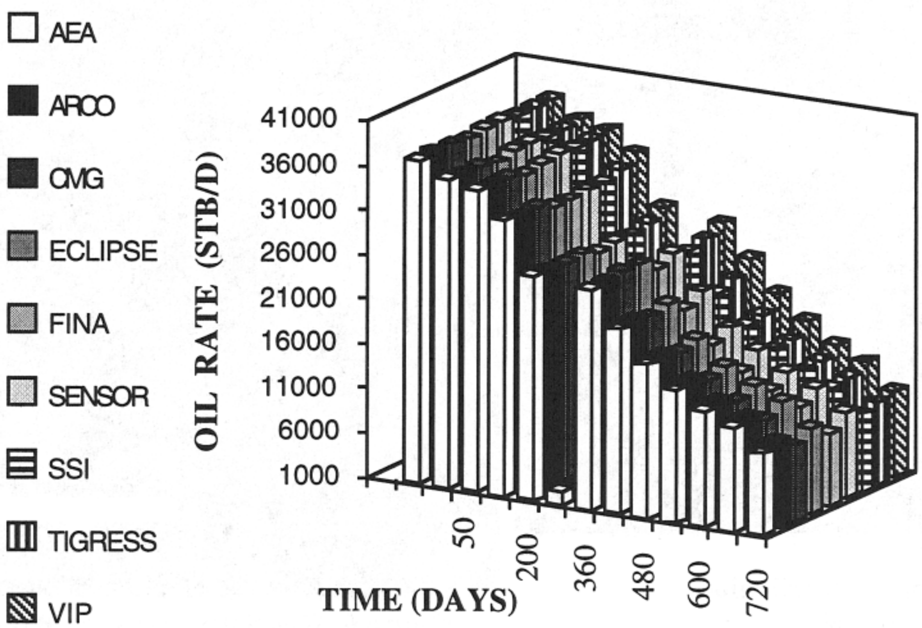


**FIGURE 9: COMPARISON OF FIELD GAS RATES**

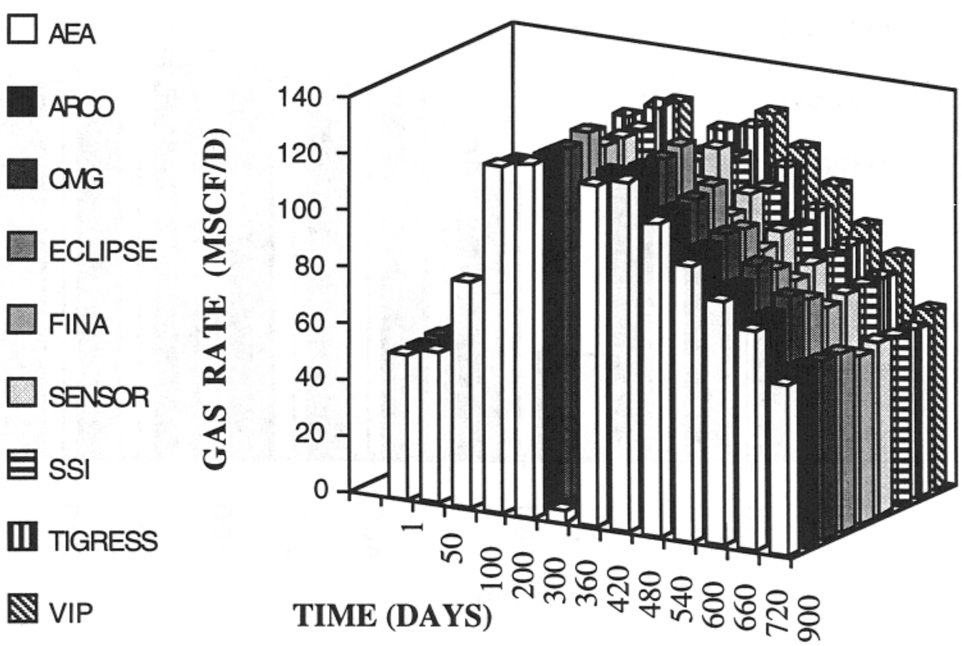

**FIGURE 10: COMPARISON OF FIELD WATER RATES**

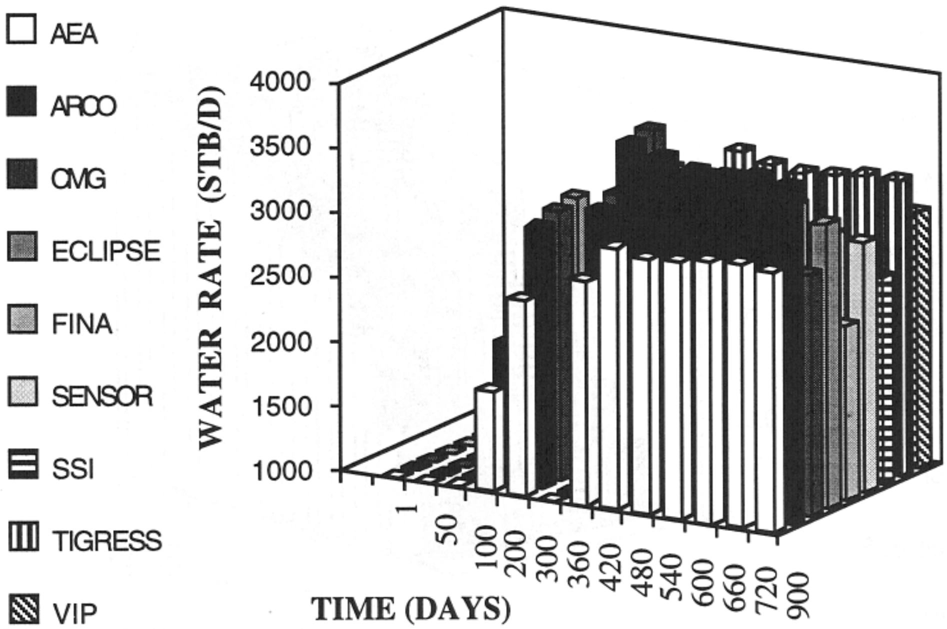


**FIGURE 11: COMPARISON OF FIELD PRESSURES AT 1,1,1**

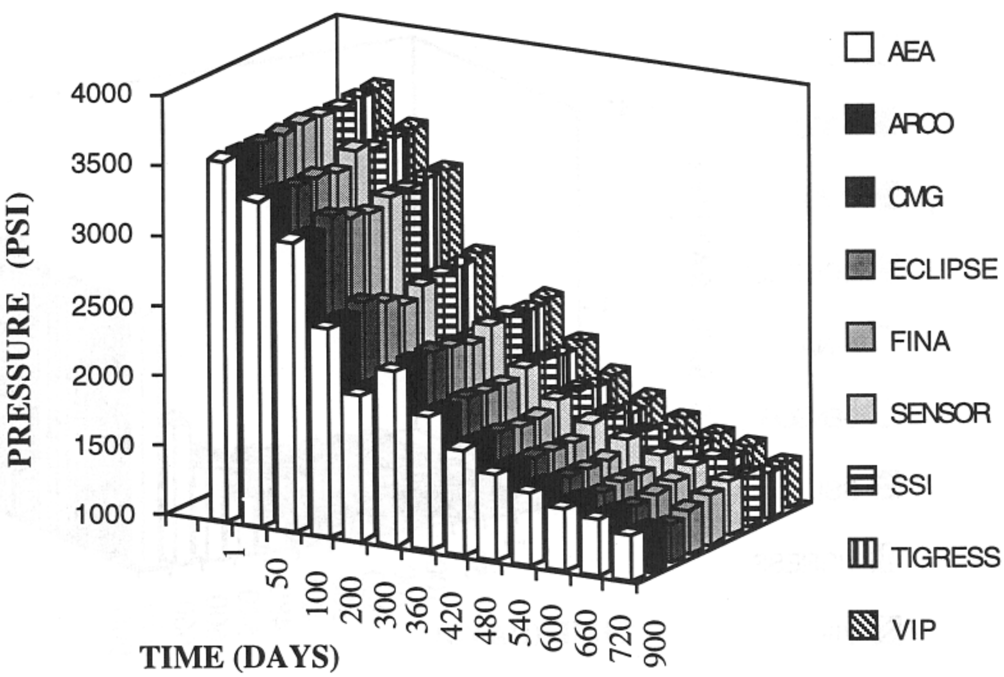

**FIGURE 12: COMPARISON OF GAS SATURATIONS AT 1,13,1**

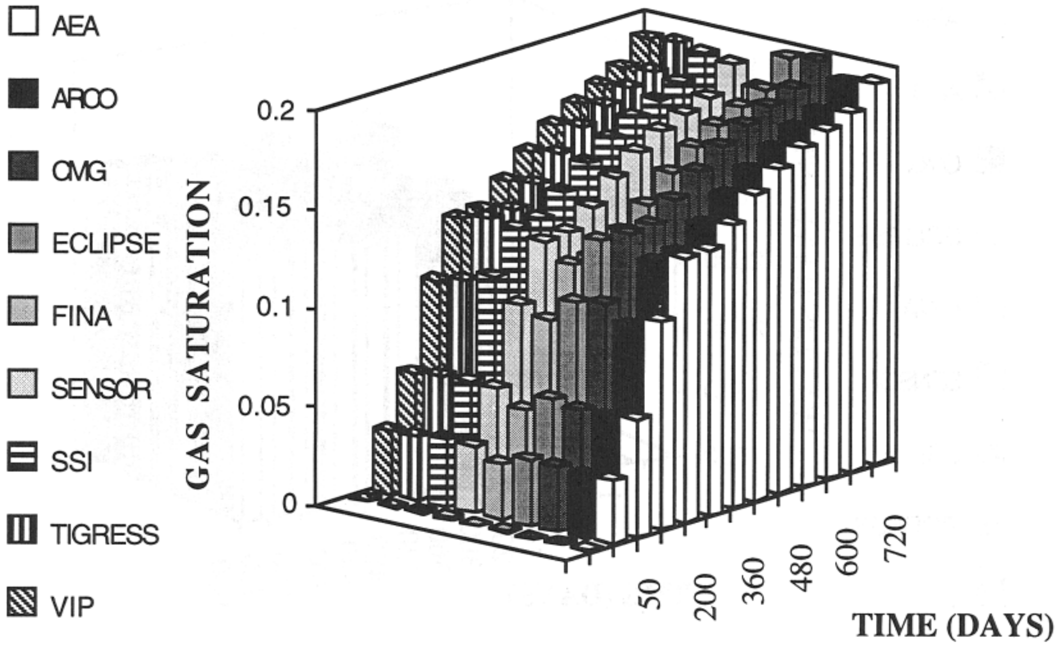


**FIGURE 13: COMPARISON OF WATER SATURATIONS AT 10,25,15**

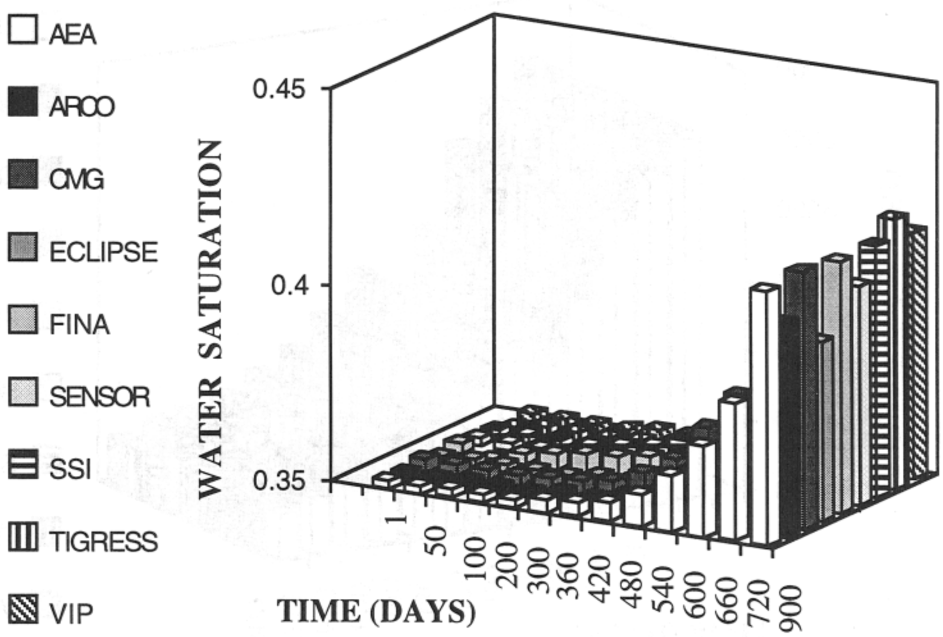

**FIGURE 14: COMPARISON OF WATER INJECTION RATES**

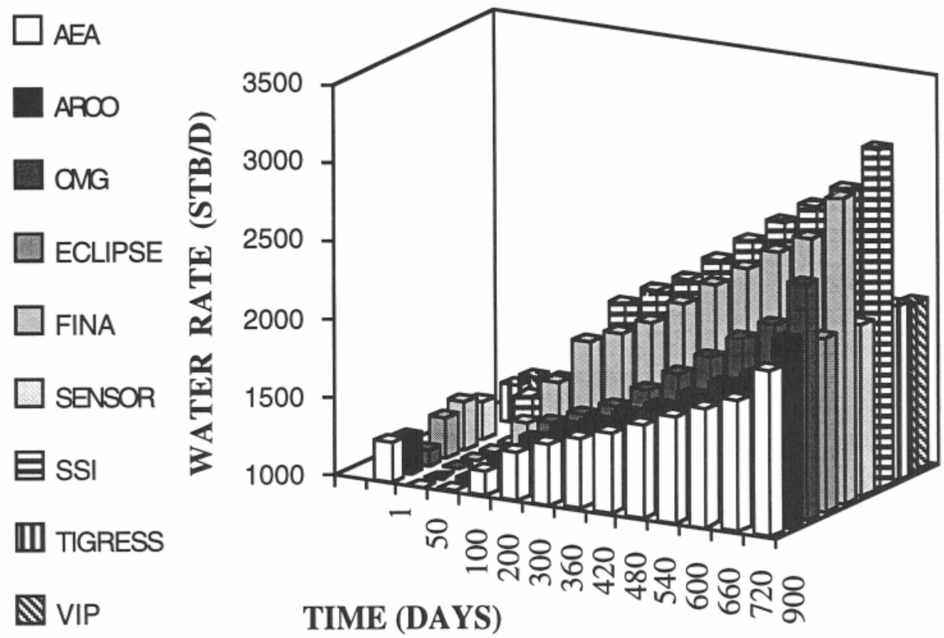


**FIGURE 15: COMPARISON OF OIL RATES FOR WELL 21**